RECRYSTALLIZATION AND WORK-HARDENING PREDICTION DURING FORGING PROCESS OF INCONEL 718

B. Marty*, J.Y. Guedou*, P. Gergaud**, J.L. Lebrun***

* Laboratoire matériaux et procédé, SNECMA, 291 av. d'Argenteuil, 92231 Gennevilliers, France

** Laboratoire des matériaux organisation et propriétés, MATOP, URA CNRS 1530, Fac. des sc. St Jérôme, 13397 Marseille, France

*** Laboratoire de mécanique et microstructure des matériaux, ENSAM, URA CNRS 1219, 151 Bd de l'Hopital, 75013 Paris, France

Abstract

The numerical simulation of forging process allows to know the temperature and strain evolution in every point of the part. The metallurgical models are able to account of these evolutions in order to predict the grain size everywhere in the work piece. The aim of the present study is to predict the recrystallized fraction in various processes (hot die forging, ring rolling, or hammering). The recrystallized fraction is strongly dependent on the stored energy (work-hardening or dislocation density) contained in the material. As a matter of fact a predictive recrystallized fraction model based on dislocation density is developed. It predicts successfully the recrystallized fraction on small samples and parts. The dislocation density is connected with the broadening of (400) X-ray line profile. The line profile broadening measurement is related to the conventional 0.2% yield stress. The correlation between predicted and measured work-hardening will be done in a following work, which will enable to link the microstructure to mechanical properties and then to predict the yield stress within a numerical simulation of the forging process.

Introduction

What is the effect of forging regarding to material microstructure and thus mechanical properties? The forge worker would say that the stronger the load of the machine is the best microstructure and mechanical properties are. The engineer would say that the load depends on the metal temperature, the dies velocity and the shape of the work piece. The metallurgist would say that forging refines the microstructure and then increases the mechanical resistance. But then the question is the following: what is refining and how does it modifie the mechanical properties of forged parts. To answer this question in the case of Inconel 718 we have to consider the different scales of strengthening:

Table I Strengthening scales for nickel base alloy

| Scale | Strengthening phenomena | Example on Inconel 718 |
|-------------------------------|-------------------------------------|---|
| Atomic scale 0.3ηn 3 to 300ηm | Solid solution γ', γ'' Precipitates | Nb in (Ni, Cr, Fe) matrix Ni ₃ (Al,Ti) in (Ni, Cr, Fe) matrix |
| 50 ηm to 10μm | Dislocation, Walls, Cells | 1113(111, 11) 111 (111, 01, 120) 11111111 |
| 5μm to 200μm | Grain size | |

The phenomenon of solid solutionning and hardening precipitation are processed by the heat treatments after forging and will not be studied in this paper. The dislocation density which will be further called work-hardening of the material is very influent on strengthening. The final grain size of work-pieces results of both static grain growth and recrystallization. Regarding the grain size, refining the microstructure has a straight forward meaning. Indeed in the case of Inconel 718 the recrystallization is often observed and then the grain size decreases during the forging process.

The recrystallized fraction indicates how far the recrystallization is achieved. This parameter is linked to the dislocation density. Indeed, recrystallization needs work-hardening to be managed, and recrystallization consumes work-hardening. The dislocation density is very difficult to measure and we will use the recrystallized fraction as an indicator of the level of work-hardening. Hence we suggest in the first part a predictive model of recrystallization based on dislocation density. This model will be fitted to experimental data. The prediction of recrystallized fraction obtained on a work-piece will be compared to the obtained one. We will also suggest an experimental method to quantify the dislocation density on forged parts.

1- Experimentation

In order to build a data base, some experiments have been performed on small specimens. Four process parameters are studied: temperature, strain, strain rate, soaking time to the forging temperature. The experiments are performed in three different strain modes: torsion (20 tests), tension (15 tests), compression (32 tests). The variation ranges of the four process parameters are presented in table II. 11 compression tests are made in several steps with a soaking time between each strain step. For each type of test the samples are held 10 minutes at the testing temperature before begining the loading. The torsion test specimens are heated by induction. The homogenous region is about 30mm. The adiabatic heating of the sample during the test is lower than 8°C. At the end of the test the sample is quenched as fast as possible. Different measurements have shown that the soaking time after loading was lower than 2s. The compression tests are carried out in a isothermal device. Hence the sample temperature is

completely homogeneous before starting the test. The adiabatic heating is lower than 10°C. The time between the end of the test and quenching is lower than 1s.

Table II definition of tested domain

| Temperature (°C) | 980 | to | 1050 |
|-------------------|-------|----|------|
| Strain | 0.1 | to | 2.5 |
| Strain rate (s-1) | 0.003 | to | 2 |
| Soaking time (s) | 1 | to | 300 |
| - | | | |

The heating of the sample in the case of tension test is radiative. The thermal homogeneous region of the sample is about 20mm. The adiabatic heating is lower than 5°C. The hold time before quenching is about 1s. For each testing condition the test is described by a thermomechanical history (time, temperature, strain, strain rate) in which the adiabatic heating is included. The initial grain size is known for each testing condition.

2- Work-hardening and recrystallization modelling

2.1- Work-hardening modelling

The dislocation density (ρ) results of the competition of three phenomena: work-hardening, recovery, and recrystallization. The effect of recrystallization on dislocation density is based on the grain size evolution. Therefore only two phenomenon are taken in account in equation (1). The work-hardening depends on the dislocation density previously existing in the material and the strain rate (first term). The recovery depends on temperature and dislocation density (second term).

$$\frac{d\rho}{dt} = \mathbf{B}_1 \times \left(\sqrt{\frac{\rho}{\rho_0}} \times \dot{\varepsilon} - \mathbf{B}_2 \times \left(\frac{\rho}{\rho_0} - 1 \right)^2 \times \exp\left(\frac{-\mathbf{T}_r}{T} \right) \right)$$
(1)

 ρ_0 is the minimum dislocation density observed in a polycrystal (10¹²m⁻²), Tr is the activation temperature of recovery, $\dot{\epsilon}$ is the strain rate, T the temperature in K. B_1 and B_2 are functions of the grain size. B_1 is the kinetic of work-hardening, and B_2 is associated to the equilibrium dislocation density (i.e. when $d\rho$ =0).

$$\mathbf{B}_{1} = \mathbf{B}_{0} \times \sqrt{\rho_{r}(D_{m})/\rho_{r}(D)}$$
(2)

$$B_{2} = \frac{\exp(T_{r}/T) \times \sqrt{\rho_{r}(D)/\rho_{0}} \times \dot{\varepsilon}}{\left(\rho_{r}(D)/\rho_{0} - 1\right)^{2}}$$
(3)

$$\rho_{r}(D) = \operatorname{Ar} \times D^{\operatorname{Br}} \tag{4}$$

The parameter ρ_{Γ} is the reference dislocation density for one couple (temperature, strain rate). $D_{\rm m}$ is the maximum grain size (200 μ m for Inconel 718) and D is the current grain size in μ m. We make the assumption that the reference dislocation density (ρ_{Γ}) is a function of grain size (equation 4). Ar and Br are parameters defined (see further) in such a way that the reference dislocation density increases with the grain size. The evolution of D while the recrystallized fraction goes increases from 0 to 1 is described in section 2.2. The relationship between flow

stress and dislocation density is described by the form $\sigma = K \times \rho^{1/2}$ where K is constant value for one material [1]. We plot on figure 1 the square root of dislocation density versus strain.

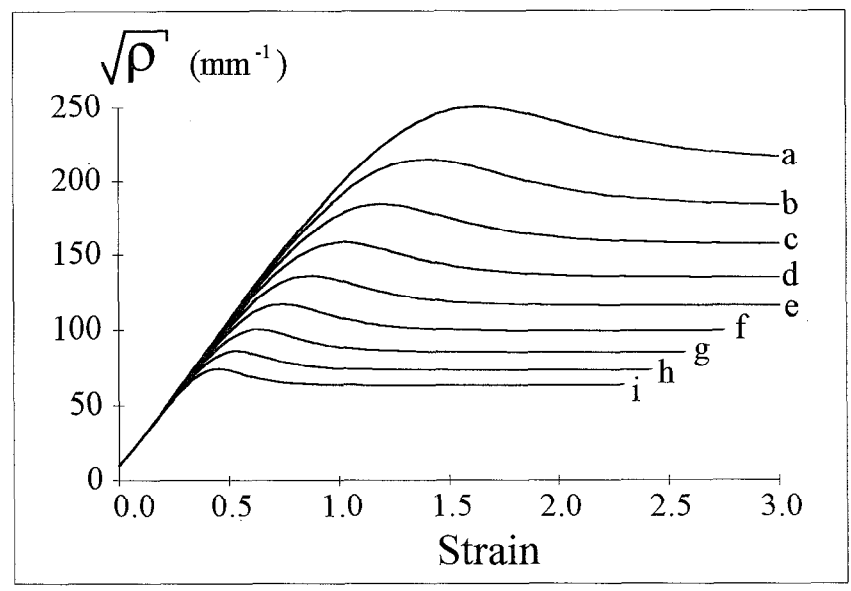


Figure 1: Evolution of the square root of dislocation density for different strain rates 0.1 (a), 0.06 (b), 0.04 (c), 0.025 (d), 0.016 (e), 0.010 (f), 0.006 (g), 0.004 (h), 0.002(i).

The evolution of simulated dislocation density with strain is coherent with the usual stress/strain plots for Inconel 718. Nevertheless the relationship between experimental stress and the square root of dislocation density is not fully verified (correlation 0,83). A possible explanation to this phenomenon is that the dependency of work-hardening and recovery with dislocation density in equation 1 is not representative of the active mechanisms in the material for a fully recrystallized structure.

2.2- Recrystallization modelling

The recrystallization phenomenon on Inconel 718 is based on nucleation and grain growth. The nucleation is supposed to occur simultaneously over the whole grain boundary. The recrystallized structure is represented by a set of very small grains of stable size. The volume occupied by this stable structure increases with the motion of the boundary between recrystallized and hardened structure.

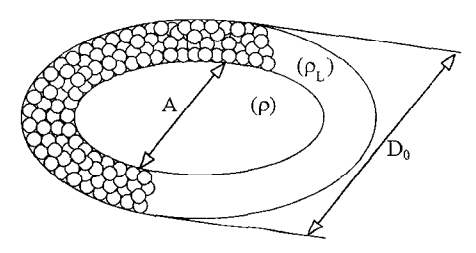


Figure 2: Schematic representation of recrystallization phenomenon.

In the case of spherical grains the surface of the grain boundary that contributes to recrystallization is $\pi \cdot A^2$ with A the hardened grain diameter. During the recrystallization, the current hardened grain size is equal to $D_0 \times (1-X)^{1/3}$. D_0 is the initial grain size of the structure. In order to describe what happens in the case of ring rolling, the recrystallization

modelling needs to work continuously from dynamic mode (recrystallization during strain) to metadynamic mode (recrystallization after strain). The grain boundary speed depends on the temperature and the difference of elastic energy between the hardened grains and the recrystallized ones (see figure 2). The difference of elastic energy between both structures is implemented in the model (5) only if it is positive.

In the hardened structure the dislocation density is continuously (in dynamic and metadynamic phases) calculated according to equation (1). In the recrystallized structure the dislocation density is not the same in dynamic recrystallization and metadynamic recrystallization. In metadynamic mode the dislocation density is assumed to be equal to the minimum dislocation density ρ_0 . Actually the recrystallized structure requires a time of recovery to reach this value of dislocation density. Due to the small grain size of this structure, we assume that this time is so small that the structure reaches immediately the minimal value of dislocation density (step of figure2). In dynamic mode the dislocation density of recrystallized structure depends on the temperature and strain rate and its calculation is detailed further.

$$\frac{dX}{dt} = A_1 \times \frac{(1 - X)^{2/3}}{D_0} \times \exp\left(\frac{-T_x}{T}\right) \times (\rho - \rho_L)$$
 (5)

As shown in figure 2 the dislocation density gradient in the structure changes during the forging process. While the strain is applied (i.e. in dynamic mode) the maximum gradient of elastic energy corresponds to the maximum recrystallization speed (i.e. boundary speed). The speed is discontinuous when the metadynamic mode starts and the dynamic mode finishes. This is due to the corresponding step of recrystallized structure dislocation density. The recrystallized fraction is implemented with time, temperature and strain rate according to equation (5). The parameter A is equal to A1 in the case of dynamic and A2 in the case of metadynamic recrystallization. T_x is the activation temperature of recrystallization.

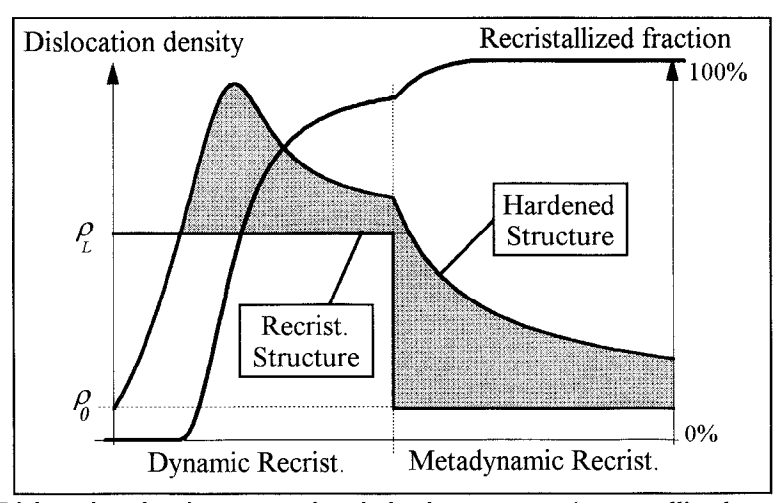


Figure 2: Dislocation density versus time in both structures (recrystallized and hardened) and in the case of dynamic and metadynamic recrystallization

In equation (5) ρ is the dislocation density resulting from equation (1). ρ_L is the dislocation density of recrystallized structure. We assume that the so called structure is composed of small grains of 1µm diameter. Its dislocation density is assumed to be also resulting from equation (1) with an infinite kinetics. We also assume that this structure has a higher temperature than the global structure. This effect is due to the elastic energy which is converted in thermal

energy while recrystallizing. The temperature gradient between recrystallized structure and hardened one is: DT. The dislocation density of recrystallized structure is given by the relation (6 solution of solution of $d\rho/dt=0$). This expression is available when the strain rate is null and then gives a dislocation density equal to ρ_0 . This allows to make a continuous description of recrystallization when starting in dynamic mode and finishes in metadynamic mode.

$$\rho_{L} = \rho_{0} \times \lim_{n \to \infty} u_{n}$$
with $u_{0} = 10$, $u_{n+1} = 1 + \omega \cdot \sqrt[4]{u_{n}}$

$$and \omega = \sqrt{\dot{\varepsilon} \cdot \exp(T_{r} / (T + DT)) / B_{2}}$$
(6)

During recrystallization, the grain size changes from D_0 to D_g (recrystallized grain size). Consequently, the constants B_1 and B_2 change. The evolution of D between D_0 to D_g is described by equation 7.

$$D = D_0 \cdot (1 - X)^{\alpha} + Dg \cdot (1 - (1 - X)^{\alpha})$$
 (7)

The α parameter allows to choose the evolution of grain size during recrystallization. This evolution is presented in figure 3 for different α parameters. The model is implemented with the time by integration of strain rate and temperature in equation (1). The recrystallized fraction results of integration of temperature and dislocation density in equation (5). This model requires the thermo-mechanical history of what the material have sustained. This history is limited to: time, temperature, strain, and strain rate. The model also requires the initial grain size before forging (D_0) .

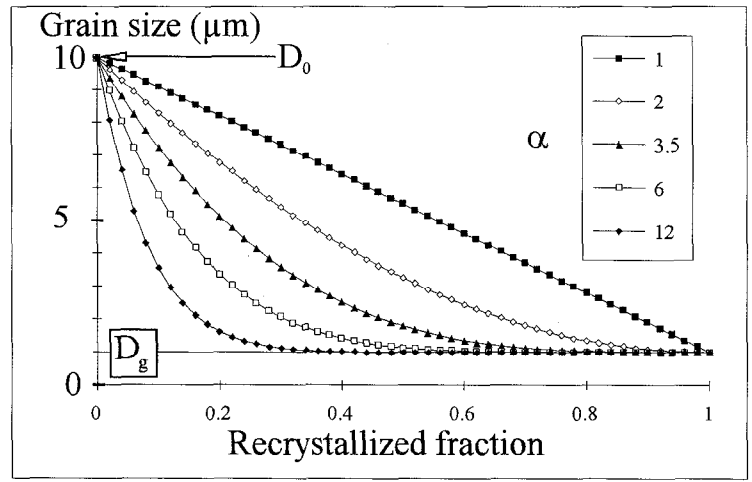


Figure 3 : Evolution of average grain size during recrystallization. (case of initial grain size of 10μm and of recrystallized grain size of 1μm)

The parameters of the model are summarised in the following list:

- T_r Activation temperature of recovery
- Ar Dislocation density of recrystallized structure (D=1µm)
- Br Sensitivity of dislocation density with grain size
- B_0 Hardening kinetics for a structure of maximum grain size (200 μ m)
- T_v Activation temperature of recrystallization
- A₁ Kinetic of dynamic recrystallization
- A₂ Kinetic of metadynamic recrystallization

The 7 parameters of the model are optimized in order to fit the experimental recrystallized fractions obtained for tests detailed in section 2. In that case the temperature Tx is equal to Tr. The adiabatic heating due to recrystallization DT is assumed to be 10° C. The α parameter is equal to 5. The model resulting from the optimised set of parameters is presented in next section.

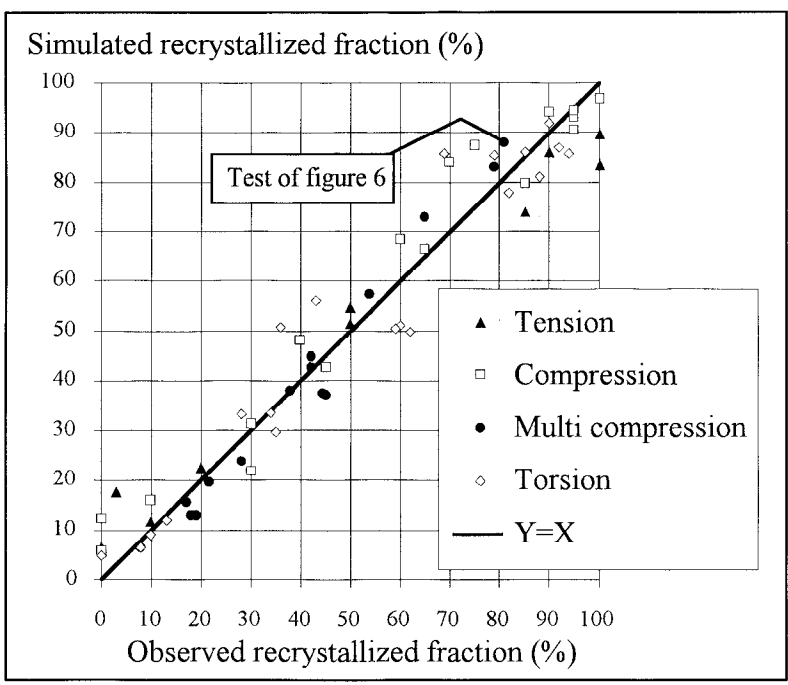


Figure 5: Predicted recrystallization fraction versus observed recrystallized fraction.

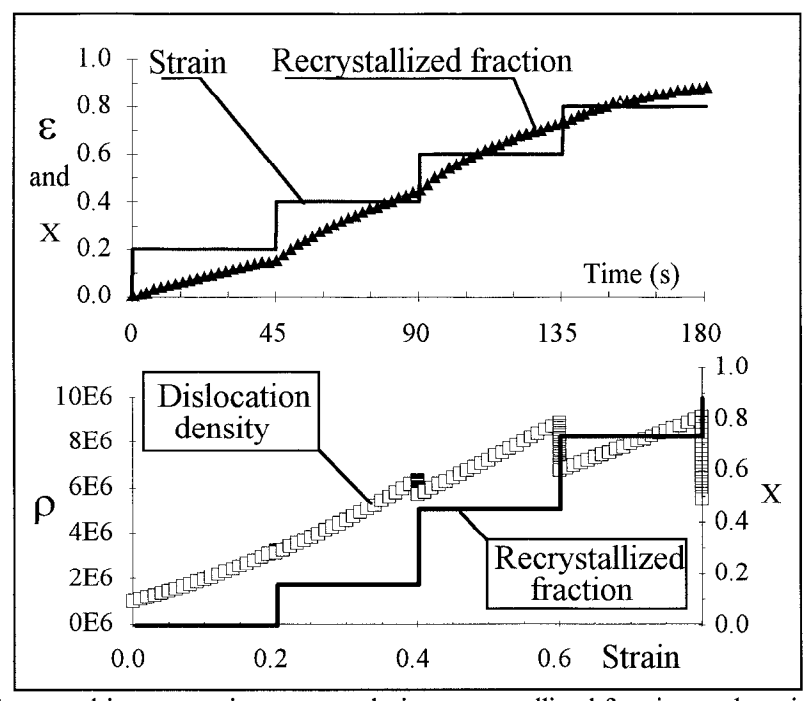


Figure 6: For a multi compression test, evolution recrystallized fraction and strain versus time (upper curves) and dislocation density and recrystallized fraction versus strain (lower curves).

3- Validation of recrystallization fraction prediction

3.1- Fitting of the model on the data base

The model parameters are optimized in order to get the best fit of experimental recrystallized fraction. The results are presented in figure 5. We can see a very good agreement between predicted recrystallized fraction and experimenal values for the various tests described is section 1. The prediction is independent of the test type. The results of the model fitting are very dependant on the description of the test by a thermo-mechanical history.

The recrystallized fraction resulting from the tension test is under-estimated by the model for the higher values. In these tests the recrystallized fraction is due to a long soaking time after deformation. The reason of the under-estimation could be that the kinetic of recovery is too high (activation temperature of recovery 44750 K). An example of model prediction is presented in figure 6. The evolution of recrystallized fraction with time shows an increase only during soaking times. Actually, during the forging steps, the dislocation density of hardened structure is at a lower level than the dislocation density of recrystallized structure (i.e. the difference $\rho - \rho_L$ is negative and then not implemented). We can also observe that the recrystallization rate decreases with the soaking time. This is associated to recovery.

3.2- Validation of recrystallization on forged parts

For different work-pieces a thermo-mechanical simulation (including metallurgical evolution) is performed with the FORGE2 code [5]. The whole forging route (from heating to quenching) is described by the simulation. For different points corresponding to the ones observed in the cut parts, the thermo-mechanical history is calculated by the software. The model is run on these data and the comparison between experimental and predicted recrystallized fractions is presented in figure 7.

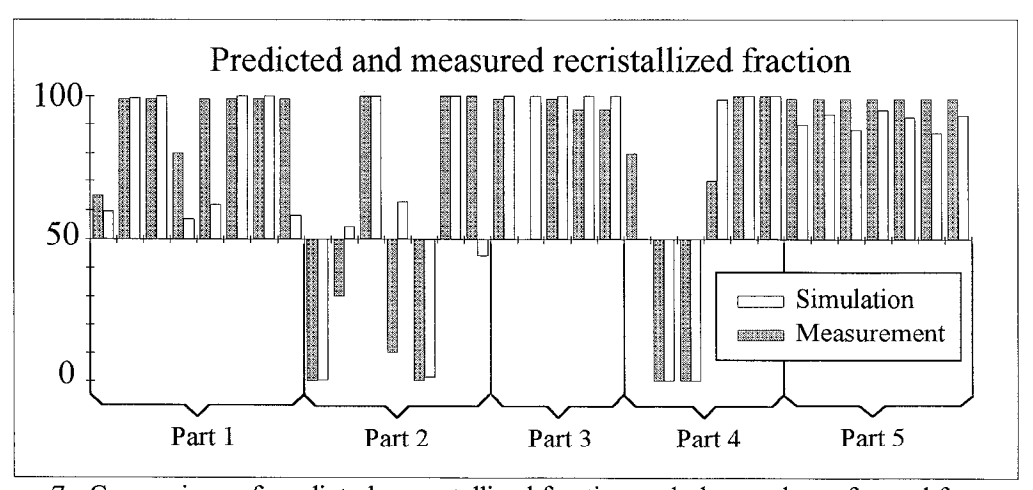


Figure 7: Comparison of predicted recrystallized fraction and observed one for real forge parts

The recrystallized fraction is rather well estimated by the predictive model (figure 7). Actually the completely recrystallized fraction are well predicted and the no-recrystallized one are also adequately accounted of. Nevertheless, in some cases, the predicted recrystallized fraction exhibits a difference with the observed one. The associated microstructure is a partially recrystallized microstructure. This microstructure is generally located close to the skin of forged parts (the inner volume of them is recrystallized and the outer areas are not recrystallized). In this area of the work piece the thermal gradient is very high and a variation

of 2 or 3 millimeters can lead to variation of 10 to 30 °C. As the model is very sensitive to temperature, the result is unstable in this area. The second reason why the results on large work pieces could not be as good as on the small samples is that the temperature exchanges with the dies is not perfectly taken into account in the current FORGE2 simulation. Then the accuracy of temperature in the skin area of work pieces is not as good as it is on small samples. To conclude with prediction of recrystallized structure on work pieces we can say that the developed model is good enough to predict the phenomenon on Inconel 718 parts.

4- Experimental determination of dislocation density and yield stress prediction

The prediction of grain size and recrystallized fraction is not sufficient to predict the mechanical properties of Inconel 718. In fact the dislocation density has a strong effect on mechanical characteristics. The aim of this work is to evaluate the dislocation density and to try to correlate it to the mechanical characteristics. The samples of Inconel 718 have been taken from disks of SNECMA forge workshop production. After forging, some of the parts are solution treated (1h to 955°C) before ageing (8h to 720°C - 2h to go to 620°C - 8h to 620°C) and some others are directly aged. For each of the 29 samples X-ray line profile analysis is performed on the head of tension test specimen. Only four direct aged samples are analyzed. They are cut in the same part at the same distance from the disk axe. This experiment will give an information about the stability of experimental measurement.

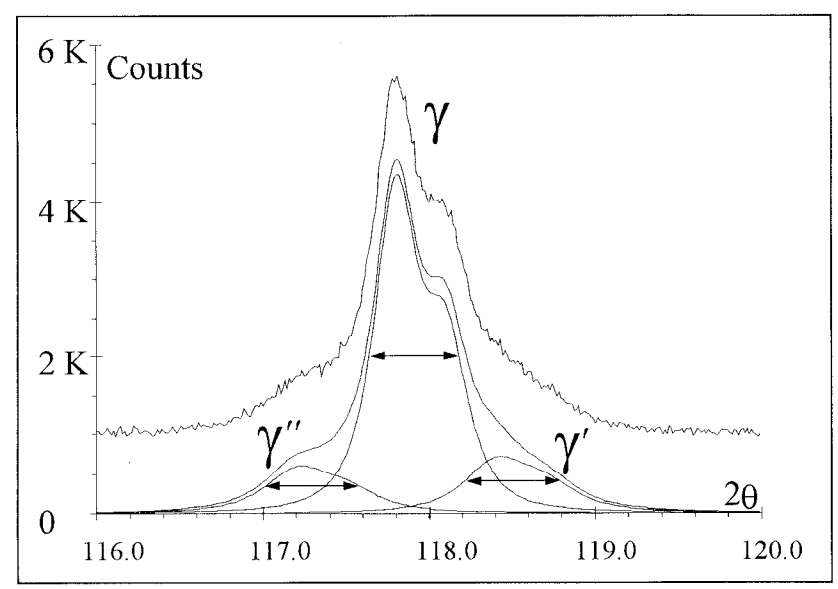


Figure 8: Fitting of the (400) x-ray line profile on Inconel 718 by a numerical function.

The conventional 0.2% yield stress is used as mechanical indication of dislocation density. The X-ray line profile analysis is used to characterize the dislocation density. The line profile analysis is performed on the (400) diffracting plane. The Copper radiation and a Germanium detector are used. The records are done from $2\theta = 113.8^{\circ}$ to 121.8° with an increment step of 0.04° . The instrumental line broadening is obtained by a numerical simulation [6,7]. This component of the broadening combines the radiation broadening and the geometrical effects of divergence. The fitting of experimental data is done by rebuilding the theoretical line profile and comparing it to the raw data. This rebuilding includes: {1} the unknown material broadening component, {2} the known instrumental broadening, {3} the K_{α} doublet, and {4} the Lorentz - Polarisation factor.

The used criterion (Sp) for the fitting is based on a statistical analysis [8]. In the case of perfect description of the raw data by the calculated function, the criterion should be centred with a standard deviation of 1. This criterion is independent of counting time. If the calculated function is far from the raw data the sensitivity of the criterion is very high. An example of fitting is presented in figure 8.

The diffraction peak associated with the (400) of Inconel 718 is actually formed of three peaks associated with the matrix and the two phases that contribute to the mechanical properties. The most important phase in term of volume and influence is the γ'' phase (Ni3Nb). The corresponding diffracting peak is placed at the left of the one associated to the γ matrix. The γ' phase (Ni3(Al or Ti)) has an effect on the stability of microstructure. The corresponding peak is at the right of the γ peak. The γ matrix is described by two peaks at the same position but with two different width representing both fractions of matrix with different work-hardenning.

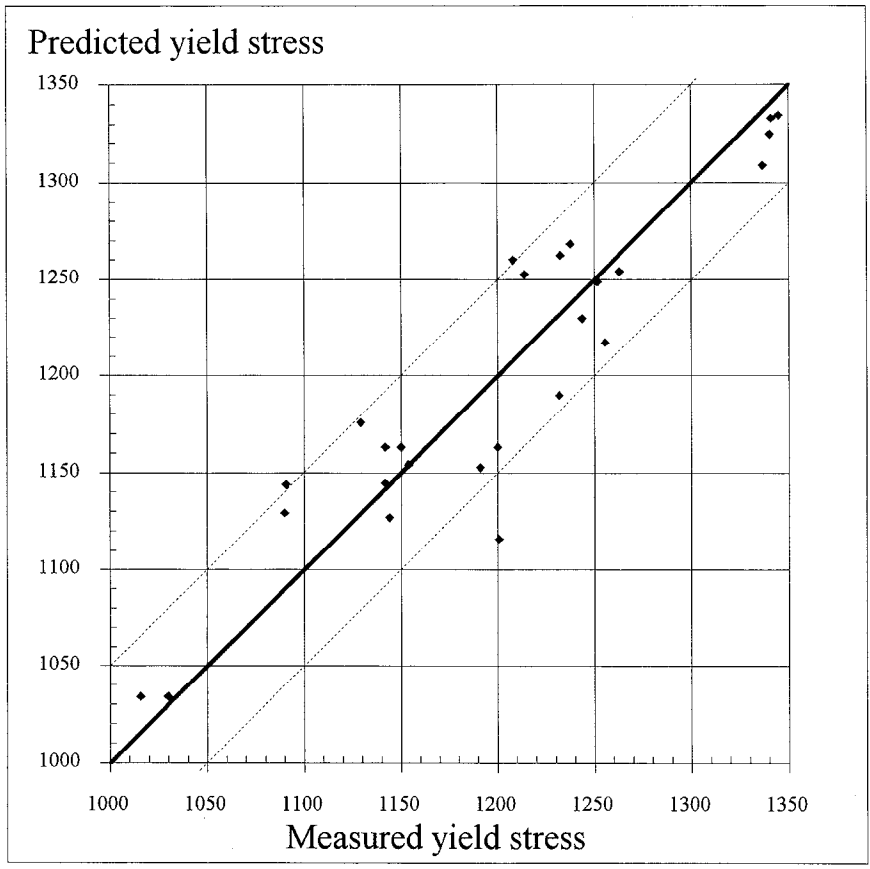


Figure 9: Predicted yield stress versus measured one.

The same numerical treatment is applied to different recorded data. From all the parameters obtained after fitting of the peak only two reduced parameters are analysed. The parameters available after fitting are the width of γ peak (β of both peaks representing the matrix: surface divided by height), the relative area of γ'' peak (β'' area of γ'' peak divided by total area). The measured grain size according ASTM standard is obtained by optical observation. This parameter called ASTM is added to the two parameters β and β'' in equation (8) to predict the yield stress of Inconel 718.

$$Re_{0.2\%}^{Predicted} = \sigma_0 + A \times ASTM + B \times \beta + C \times f''$$
 (8)

The four constants σ_0 , A, B, and C are respectively equal to 582 MPa, 30.6 MPa, 20 MPa· μ m, and 372 MPa. The first constant is very similar to the minimum yield stress on Inconel 718 (large grains, low dislocation density, no γ'' and γ' phase). On the 29 samples, the range of variation of the different parameters is $\{8.1 \text{ to } 21.2\}$ for β in μ m-1, $\{6.1\%$ to $26.0\%\}$ for f', and $\{8 \text{ to } 13\}$ for the grain size. Figure 9 shows the rather good agreement between measured and predicted yield stress.

The predicted yield stress is only based on microstructure description. The good correlation of the predicted yield stress to the mechanical properties of Inconel 718 shows that the three parameters that have been chosen to describe Inconel 718 microstructure are influent parameters on mechanical properties. The prediction that has been developed is able to separate three types of microstructures: the one leading to very high yield stress (1250-1350 MPa), the one leading to medium yield stress (1125-1225 MPa), and the one leading to very low yield stress (1000-1100 MPa). One limitation of this yield stress prediction is due to the grain size optical determination. Actually in some microstructural cases the ASTM parameter is not easy to measure because of numerous twins in the microstructure. The heterogeneous structure of Inconel 718 is also a problem to quantify this grain size. And finally the scale of observation is a problem because it does not allow to observe the dislocation cells of the material which may be a more relevant parameter than the metallographic grain size. For all these reasons a cristallite (coherent diffracting domain) size observation is being developed to characterize the microstructure by a parameter representative of the material at a small scale, relative to a large sampling volume of it (volume observed $5\times5\times0.01$ mm³), and independent of human observation.

Conclusion

The aim of the present work was to describe the forged alloy Inconel 718 at a very local level (scale of dislocation). In the mean time the purpose of the study was to describe this very high complexity with a rather simple and then usable in a forge workshop model. The main conclusions of this work can be summarised as follows:

- 1- A recrystallization model based on dislocation density has been developed and predicts successfully this microstructural parameter on forged parts as well as on small specimens. The model is based on two coupled differential equations that are introduced in FORGE2 software.
- 2- The dislocation density predicted by the model has not been validated because of difficulties to measure it on such heterogeneous structure. Nevertheless the shape of plots representing the square root of dislocation density versus strain are rather close to the one expected.
- 3- A dislocation density determination is suggested by x-ray line broadening analysis. This determination integrates a large volume of the material $(5\times5\times0.01\text{mm}^3)$ which makes it adequate for industrial application. It requires a very simple preparation which makes it usable in a workshop environment.
- 4- For various microstructures on Inconel 718, the breadth of analysed x-ray line which is representative of dislocation density is integrated in a predictive model of conventional 0.2% yield stress. This model predicts successfully the yield stress within ±50MPa for a range of 350MPa. The established link between microstructure and mechanical properties which is already interesting should be improved by a crystallite size measurement by x-ray analysis.

The relationship between predicted and measured dislocation density will be done in a subsequent work in order to link the microstructural parameters predicted by FORGE2 to mechanical properties. It will be then possible to predict directly the yield stress of Inconel 718 with a numerical simulation of forging process.

References

- [1] F. Haessner, <u>Recrystallization of metallic materials</u>, (Dr. Riederer-Verlag GMBH Stuttgart, 1978)
- [2] F.J. Humphreys, and M. Hatherly, <u>Recrystallization and related annealing phenomena</u> (Pergamon, 1995)
- [3] Y. Desvallées, M. Bouzidi, F. Bois, and N. Beaude, Delta phase in Inconel 718: Mechanical properties and forging process requirements, Superalloys 718, 625, 706 and various derivatives, Edited by E.A. Loria, The minerals, Metals & Materials society, 281-291, 1994
- [4] J.Y. Guedou, G. Simon and J.M. Rongvaux, Development of damage tolerant Inconel 718 for high temperature usage, Superalloys 718, 625, 706 and various derivatives, Edited by E.A. Loria, The minerals, Metals & Materials society, 509-522, 1994
- [5] B. Glut, T. Coupez and J.L. Chenot, Automatic mesh generator for complex 2D domains. Application to moving geometries in forming processes, J. of Mat. Proc. Technology, 69-76, 1993
- [6] B. Marty, Metallurgical study of 718 alloy by x-ray line profile analysis, (Doctorate Thesis, Paris, ensam, 1996)
- [7] B. Marty, P. Gergaud, B. Bourniquel, J.L. Lebrun, X-ray instrumental broadening: simulation, fitting and convolution with material component profile, (to be published. 1997)
- [8] B. Bourniquel, Fourth international conference on residual stresses, Proceeding edited by M.R. James, 269-276, 1994